8.9 Object Kinetic Monte Carlo Simulations of Cascade Annealing in Tungsten —

G. Nandipati, W. Setyawan, H. L. Heinisch, K. J. Roche, R. J. Kurtz (Pacific Northwest National Laboratory) and B. D. Wirth (University of Tennessee)

OBJECTIVE

The objective of this work is to study the annealing of primary cascade damage created by primary knock-on atoms (PKAs) of various energies, at various temperatures in bulk tungsten using the object kinetic Monte Carlo (OKMC) method.

SUMMARY

We used our recently developed lattice based object kinetic Monte Carlo code; KSOME [1] to carryout simulations of annealing of individual displacement cascades in bulk tungsten that were generated using molecular dynamics (MD) simulations, at temperatures of 300, 1025 and 2050 K and PKA energies up to 100 keV. We find that at smaller PKA energies the fraction of surviving self-interstitial atoms (SIAs) and vacancies decreases with temperature, whereas at higher PKA energies the fraction of surviving defects at first decreases and then increases with temperature.

PROGRESS AND STATUS

Introduction

Tungsten is considered as the primary material choice for divertor components in future fusion reactors due to its high melting point, low sputtering coefficient, high thermal conductivity, low transmutation probability, low tritium retention and good mechanical strength. Bulk tungsten will be exposed to energetic neutrons escaping the plasma. The deuterium-tritium fusion reaction produces neutrons with a characteristic kinetic energy of 14.1 MeV. Collisions of 14.1 MeV neutrons with tungsten atoms produce tungsten primary-knock-on atoms with various recoil velocities. PKA atoms then lose the acquired energy to a large extent by displacing other atoms, in a sequence known as a displacement cascade. The whole process lasts for up to tens of picoseconds, and the debris left behind consists of point defects and clusters concentrated in a small volume, called primary damage.

MD has been used extensively to study the primary damage in materials. However, due to the requirement of femtosecond time steps in MD, long-term defect evolution is beyond its scope. Therefore the OKMC code, kSOME was used to carry out annealing simulations of primary damage. These simulations were intended to be an extension of MD simulations in time-scale. Accordingly, the OKMC method is used to carry out annealing simulations at exactly the same temperature at which the cascades were generated with MD, using a big simulation box. The purpose of the current work is to use the OKMC method to carry out annealing simulations of primary damage in pure tungsten produced by PKAs up to 100 keV at temperatures of 300, 1025 and 2050 K.

[1] PNNL is operated for the U.S. Department of Energy by Battelle Memorial Institute under Contract DE-AC06-76RLO 1830.

Simulation Details

Simulations were performed on a cubic block of tungsten atoms having a side length of 512 lattice units or 162 nm, with each axis parallel to a <100> direction of the crystal. In tungsten, cascades are compact, and the volume of the simulation box chosen is large enough that we expect the results to be insensitive to the box size. Each atom is allowed to hop to one of eight body-centered cubic nearest neighbor lattice sites at *a*/2 (111), where *a* is the lattice constant. Initial defect distributions of SIA and vacancy defects obtained from MD cascade damage simulations were placed in the center of the box. Absorbing boundary conditions were adopted in all three directions i.e., when a defect diffuses out of the box it is no longer tracked and is removed from the simulation. Such defects are counted as escaped defects and contribute to long-range defect diffusion. These defects will interact with the rest of the microstructural features leading to microstructural changes and damage accumulation.

The values of migration energies and pre-factors for diffusion and binding energies of defects used in our annealing simulations are taken from the *ab initio* calculations of Becquart *et al*. [3]. In the present model SIA clusters larger than size five were constrained to diffuse in 1-D along one of four <111> directions. While SIA clusters up to size five were allowed to change their direction of 1D motion via rotation and thereby perform mixed 1D/3D motion. Activation barrier for changing the direction of their 1D motion from one <111> direction to another is 0.38 eV. Since MD does not provide information on the orientation of SIA diffusion, the direction of 1D motion was assigned randomly to the SIAs at the start of a simulation. Also there is no information available on infrequently occurring immobile SIA clusters in these cascades therefore we assumed that all interstitial clusters are glissile (mobile). Their migration/diffusion rates decrease with increasing cluster size (n) according to $n_o n^{-a}$ ($n_o = 6 \times 10^{12}$ s^{-1}, a = 0.5).

For a single vacancy, the activation barrier for diffusion is taken as 1.66 eV, and vacancy clusters larger than five are assumed to be inactive i.e., they neither diffuse nor emit, although they interact with other defects if they are within the range of interaction. All vacancies migrate in 3D, and their diffusion rates decrease with cluster size (n) according to $n_o(q^{-1})^{n-1}$ ($n_o = 6 \times 10^{12}$ s^{-1}, q = 1000). The vacancy (SIA) dissociation rate is given by $G_d = n_d \exp((E_m + E_d)/k_B T)$, where E_d is the binding energy of a vacancy (SIA) to a vacancy (SIA) cluster, and E_m is the migration energy of a single vacancy (SIA). We have assumed that defect clusters of all sizes are spherical objects and their capture radii were also obtained from Reference [3].

Table 1. Average number of surviving Frenkel Pairs in tungsten from MD simulations as a function of PKA energy and temperature [2].

PKA Energy (keV)	TEMPERATURE (K)		
	300	1025	2050
10	12	9.3	9.3
20	22.1	18	15
30	29.6	22.4	21.7
40	34.7	31.7	32.3
50	50	43	38.1
60	60.8	52.7	50.7
75	81.3	80.5	72.9
100	116.3	110.5	100.3

RESULTS

A database of 15-20 cascades at PKA energies ranging from 10 keV to 100 keV was created using MD simulations. With each MD cascade, i.e. the same PKA energy, the same location and the same direction, we carried out 20 runs with different random seeds. Results presented here were averaged over both different cascades and random seeds. Thus each data point in the plots shown in this report was averaged over 300-400 runs. Simulations were carried out at temperatures of 300, 1025 and 2050 K for up to 10 ns. Note that 1025 K and 2050 K correspond to 0.25 and 0.5 of the melting temperature of tungsten respectively (from the interatomic potential). We have also carried out simulations longer than 10 ns, but due to fast interstitial diffusion rates we found that almost all of the recombination and coalescence events happen in the very first few nanoseconds (ns) of the simulation, therefore we only show results up to 10 ns for all temperatures and PKA energies. Beyond 10 ns we find the most frequent events are interstitial clusters escaping the simulation box. To understand the annealing of single cascades in tungsten we have also collected runtime information like number densities of defects, reaction events (recombination, coalescence, emission, transformation), average cluster sizes and their size distributions, and number densities of defects escaping the box for all the types (in our case they are only SIAs and vacancies) as a function of time. Information about the details of MD simulations carried out to generate the database of cascades and other additional details about the cascades can be found in Reference [2]. Table 1 shows the average number of Frenkel pairs for 300, 1025 and 2050 K at various PKA energies. The number of Frenkel pairs increases with PKA energy and decreases very slightly with temperature. To compare annealing of cascades across different PKA energies and temperatures, the number of surviving defects was normalized by the average number of defects at the start of the simulation.

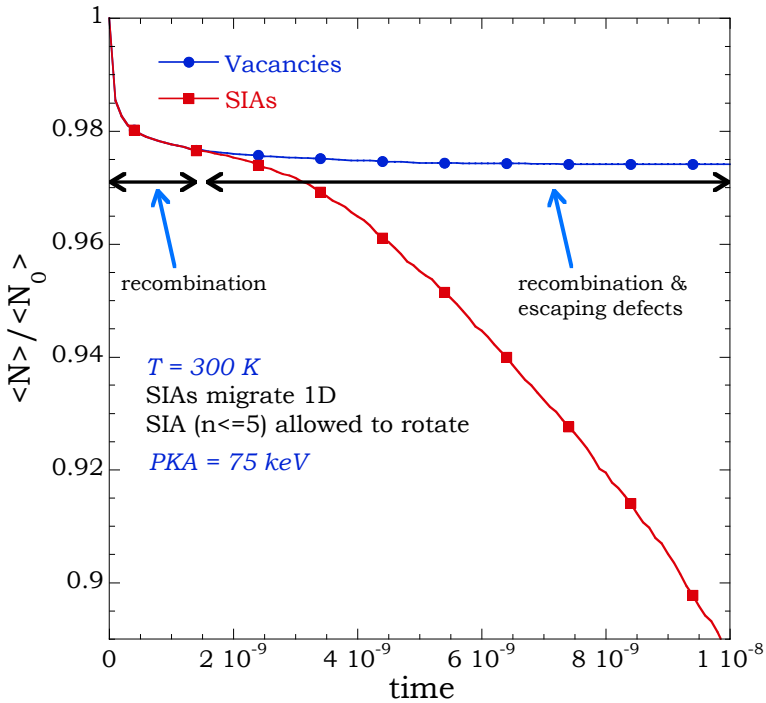

Figure 1. Normalized surviving fraction of SIAs and vacancies as a function of time for a PK of 75 keV and at 300 K.

Figure 1 shows a plot of the surviving fractions ($n_d = \sum nS_d$, n = number of defect clusters of size S_d) of all SIAs and vacancies as a function of time for a PKA energy of 75 keV at 300 K. This plot shows all the features of defect evolution common to all PKA energies and temperatures. One can see from Figure1 that the initial decrease in surviving defects is due to recombination only (the surviving fraction of SIAs and vacancies are equal), and this occurs in the very first few ns. As the highly mobile SIAs diffuse beyond the boundary of the simulation box, the total number of interstitial defects is no longer equal to the number of vacancy type defects, which results in a drop in the fraction of surviving SIAs (see Figure1). At 300 K, interstitials migrate very fast, and they very quickly diffuse away from the primary damage region, while the migration rate vacancy clusters is so low that they are immobile for the time-scale of the simulation and can be considered immobile for the time scales of the simulations up to 2050 K. It can be seen from Figure 1 that the surviving fraction of vacancies remains nearly constant after early recombination events. Therefore, for convenience we will show only the surviving fractions of SIAs in all the plots hereafter. As mentioned in the previous section, the emission rate is determined by the sum of binding and migration energies and this sum is large for both SIA and vacancy clusters. Therefore, for the very short time-scale of the simulation, emission is an infrequent event even at 2050 K. In our test runs to analyze different aspects of annealing we have observed that, within the simulation time of 10 ns, rotation of small SIA clusters is not very active and does not significantly affect the annealing of primary damage below 500 K. We do have results that show how cascades generated at different PKA energies anneal, but in this report we present only the temperature effects, which are much greater and even somewhat counterintuitive.

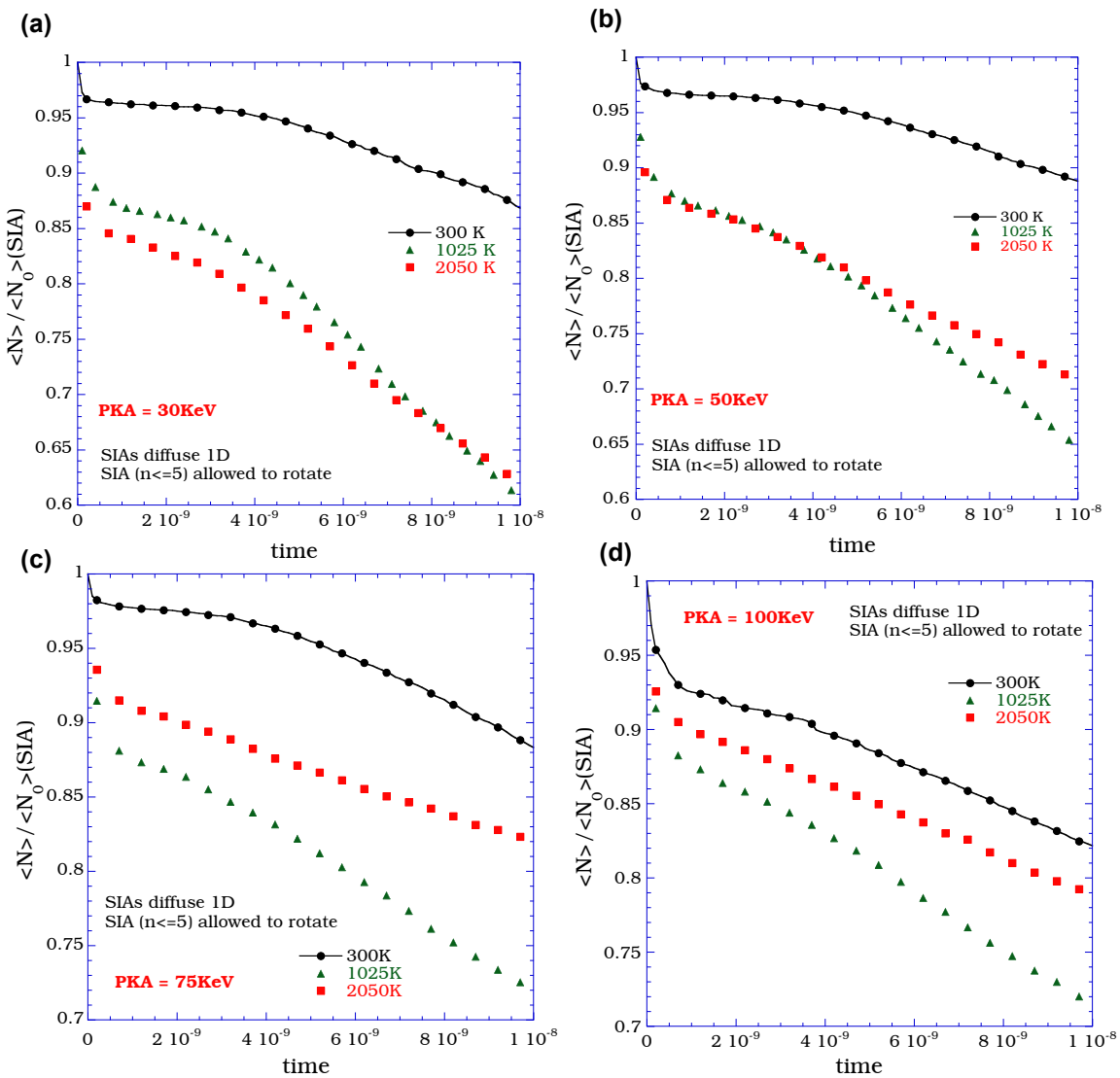

Figure 2. Effect of temperature on the normalized surviving fractions of SIAs as a function of time for cascades at PKA energies of (a) 30 keV (b) 50 keV (c) 75 keV (d) 100 keV.

Figure 2 shows the surviving fractions of SIAs in cascades as a function of time at temperatures of 300, 1025 and 2050 K for PKA energies of 30, 50, 75 and 100 keV. The results vary with increasing cascade energy. For 30 keV cascades the fractions of SIAs lost due to recombination increase with temperature (see Figure 2(a)). For cascades at 75 and 100 keV the fractions of SIAs lost to recombination increase with temperature from 300 K to 1025 K. Counterintuitively, it appears to decrease with temperature (see Figures 2(c) & (d)) and for 50 keV cascades the fraction of defects lost to recombination is almost the same at 1025 and 2050K (see Figure 2(b)). Note that the dotted line of filled red squares in Figure 2 represents the fraction of surviving SIAs at 2050 K which is in the middle of 300 K and 1025 K lines for 75

and 100 keV cascades. Another observation that can be made is that at 2050 K, for 30 and 50 keV cascades, SIAs escape the simulation box at a much slower rate than at 1025 K. We think that the reduced recombination observed at 2050 K for 75 and 100 keV cascades is due to a combination of factors like the spatial and size distributions of SIA and vacancy clusters (i.e., cascade morphology), the fast SIA diffusion rate, rotation/non-rotation of SIA clusters and, the cluster size distribution of SIA and vacancy clusters in the initial cascades.

FUTURE WORK

We intend to carry out further tests to find out what causes the reduced recombination at 2050 K during annealing of high PKA energy cascades. In addition, we intend to carry out additional simulations to test the effect of rotation/non-rotation of SIA clusters, and migration barrier of both SIA and vacancy clusters on the annealing of primary damage. In addition, we plan to perform simulations of irradiation using the same set of MD cascades at the same temperature at which they were generated and at various dose rates.

ACKNOWLEDGEMENT

All computations were performed on CARVER at National Energy Research Scientific Computing Center (NERSC).

REFERENCES

[1] G. Nandipati, *et al.,* Semiannual Progress Report DOE/ER-0313/54, June 2013, 179-183.
[2] W. Setyawan, *et al.,* Semiannual Progress Report DOE/ER-0313/54, June 2013, 200-204.
[3] C. S. Becquart, *et al., J. Nucl. Mater.* **403** (2010) 75.